

Coronary CT Angiography*

Udo Hoffmann^{1,2}, Maros Ferencik¹, Ricardo C. Cury¹, and Antonio J. Pena¹

¹Department of Radiology, Massachusetts General Hospital and Harvard Medical School, Boston, Massachusetts; and

²Harvard School of Public Health, Boston Massachusetts

Advances in multidetector CT (MDCT) technology with submillimeter slice collimation and high temporal resolution permit contrast-enhanced imaging of coronary arteries and coronary plaque during a single breath hold. Appropriate patient preparation, detailed technical and technological knowledge with regard to recognition of typical imaging artifacts (such as beam hardening or motion artifacts), and the adequate choice of postprocessing techniques to detect stenosis and plaque are prerequisites to achieving diagnostic image quality. A growing number of studies have suggested that 64-slice coronary CT angiography is highly accurate for the exclusion of significant coronary artery stenosis (>50% luminal narrowing), with negative predictive values of 97%–100%, in comparison with invasive selective coronary angiography. In addition, several studies have indicated that MDCT also can detect calcified and noncalcified coronary atherosclerotic plaques, especially in proximal vessel segments, showing a good correlation with intracoronary ultrasound. Studies on clinical utility, cost, and cost-effectiveness are now warranted to demonstrate whether and how this technique can change and improve the current management of patients with suspected or confirmed coronary artery disease.

Key Words: coronary CT angiography; coronary MDCT; coronary artery stenosis; cardiology

J Nucl Med 2006; 47:797–806

Over the last five years a dramatic improvement in multidetector CT (MDCT) technology has occurred. The ability to noninvasively image the coronary artery lumen and wall and obtain information on the presence, severity, and characteristics of coronary artery disease (CAD), including the visualization of luminal obstruction and atherosclerotic plaque, constitutes an attractive addition to currently available diagnostic tools, such as nuclear perfusion imaging or invasive selective coronary angiography, for the work-up of patients with known or suspected CAD.

This review provides detailed information on how to perform state-of-the-art coronary CT angiography (CTA)

examinations, including patient preparation, image acquisition, and evaluation techniques. In addition, the potential clinical applications and limitations of the technique are discussed.

PATIENT PREPARATION

High-quality source images are the most important prerequisite for the diagnostic assessment of coronary CTA. Image quality must be ensured through multiple steps, including patient preparation, the actual coronary CTA scan protocol, and the synchronization of raw image data with electrocardiography (ECG) information, which enables the reconstruction of axial ECG-gated images. Because the injection of iodinated contrast material is necessary to visualize the coronary artery lumen, coronary CTA is absolutely contraindicated in some subjects. Relative contraindications exist with respect to conditions that are known to limit diagnostic image quality. Table 1 summarizes absolute and relative contraindications.

Premedication

The image quality of coronary CTA is substantially improved in patients with a heart rate of less than 65 beats per minute. Motion artifacts observed in patients with higher heart rates contribute substantially to the degradation of image quality. Multiple studies have demonstrated that the highest image quality of coronary CTA for current generations of 16- and 64-slice MDCT scanners can be achieved at low heart rates (<65 beats per minute) (1–3).

Recent investigations have demonstrated that heart rate is decreased by approximately 6 beats per minute as a result of the inspirational breath hold only (4). Therefore, aggressively reducing a patient's heart rate before a scan is advised for patients with a heart rate of more than 70 beats per minute. The most common approach in current clinical practice is the administration of an oral β -blocker (50–100 mg of oral metoprolol is administered 1 h before the scan) or an intravenous β -blocker (5–20 mg of intravenous metoprolol is administered immediately before the scan) with a short half-life (5–8). Our recent experience with 150 subjects referred clinically for coronary CTA indicates that intravenous metoprolol in combination with the effect of the breath hold leads to a reduction in the heart rate by an average of 11 beats per minute (4). Alternatively, calcium

Received Jan. 23, 2006; revision accepted Mar. 13, 2006.

For correspondence contact: Udo Hoffmann, Department of Radiology, Massachusetts General Hospital and Harvard Medical School, 165 Charles River Plaza, Suite 400, Boston, MA 02114.

E-mail: uhoffman@partners.org

*NOTE: FOR CE CREDIT, YOU CAN ACCESS THIS ACTIVITY THROUGH THE SNM WEB SITE (http://www.snm.org/ce_online) THROUGH MAY 2007.

TABLE 1

Absolute and Relative Contraindications for Coronary CTA

Contraindication	Description
Absolute	Hypersensitivity to iodinated contrast agent
Relative	History of allergies or allergic reactions to other medications
	Renal insufficiency (serum creatinine level of >1.5 mg/dL)
	Congestive heart failure
	History of thromboembolic disorders
	Multiple myeloma
	Hyperthyroidism
	Pheochromocytoma
	Atrial fibrillation
	Inability to perform breath hold for 15 s

channel blockers can be used to reduce the heart rate in patients with a contraindication to β -blockers.

In addition, sublingual administration of short-acting nitroglycerin (2 tablets, equal to 0.8 mg) immediately before a scan has been used to improve the visualization of the coronary artery lumen. The vasodilatory effect of nitroglycerin on coronary vessels has been studied extensively in selective coronary angiography, producing increases in luminal areas of between 20% and 40% in normal arteries and 5% and 10% in diseased coronary artery segments (9,10). Although this technique may allow for improved identification of stenosed coronary artery segments, it harbors the potential to overestimate the degree of stenosis.

Current data on the effects of nitroglycerin in coronary CTA are not available. Case-control studies are warranted to establish the benefits of the use of nitroglycerin, which include improved visualization of the coronary arteries, especially in women, subjects with diabetes, and subjects with hypertension. Nitroglycerin is contraindicated in subjects taking phosphodiesterase inhibitors, such as sildenafil or vardenafil, and in subjects with hypersensitivity to organic nitrates, increased intracranial pressure, symptomatic hypotension, and severe anemia.

Patient Positioning and Preparation for Scanning

Patients are positioned on the CT examination table in the supine position. Three ECG leads are attached to obtain an adequate ECG tracing. A noise-free ECG signal is important to synchronize the ECG signal to the raw image data. Intravenous access via a large intravenous line (e.g., 18 gauge) is necessary to ensure easy injection of the viscous contrast agent at a flow rate of 5 mL/s. Except in very obese patients, a flow rate of 4 mL/s usually renders diagnostic image quality as well.

It is important to prepare the patient for the sensations experienced from the injection of the contrast agent and to perform repeated test breath holds. We recommend the breath hold during inspiration preceded by a cycle of inspiration and expiration. This approach improves the length

and stability of the breath hold during the scan and leads to the reduction of unintentional movements during the scan, in turn resulting in better image quality. During the test breath holds, a decision regarding whether β -blocker administration is necessary can be made.

IMAGE ACQUISITION AND RECONSTRUCTION

Protocol for Spiral ECG-Gated Scan

The acquisition of the dataset for coronary CTA consists of 3 steps: topogram, determination of the adequate initiation of the coronary CTA image acquisition to ensure homogeneous contrast enhancement of the entire coronary artery tree, and coronary CTA scan. A low-energy topogram is acquired as the first step. This scan permits accurate positioning of the scan volume (Fig. 1A). Two techniques are available to determine the adequate initiation of the coronary CTA image acquisition to ensure homogeneous contrast enhancement of the entire coronary artery tree: the bolus tracking technique and the timing bolus technique.

The bolus tracking technique uses a series of dynamic low-dose axial scans (every 2 s) at the level of the carina to track the bolus of contrast material and to monitor the contrast enhancement at the level of the ascending aorta. The coronary CTA imaging sequence is initiated when the contrast enhancement reaches a predefined value, usually 100 Hounsfield units. The timing bolus technique uses a small bolus of iodinated contrast agent (10–20 mL) followed by normal saline (30–50 mL) injected into the antecubital vein at a rate of 4–5 mL/s (Fig. 1B) to determine the contrast material transit time. An ungated axial image is generated every 2 s at the level of the ascending aorta. The time from the start of the injection to the peak contrast enhancement in the ascending aorta determines the scan delay after the initiation of contrast material administration. The timing bolus technique (11–17) and the bolus tracking technique (18–22), if performed correctly, provide similar results and have been applied successfully in multiple research studies.

In the third step, a CT volume dataset for the coronary arteries is acquired; this dataset covers the entire heart from the proximal ascending aorta (approximately 1–2 cm below the carina) to the diaphragmatic surface of the heart. The scan is acquired in a single breath hold during comfortable inspiration and starts with the injection of a contrast agent with a high concentration of iodine (300–400 mg/mL) at a high flow rate (4–6 mL/s). The total volume of contrast agent depends on the scan length, but typically 60–80 mL are injected, followed by a saline bolus (40–70 mL at 4–6 mL/s). The actual CT scan starts after the delay calculated as the contrast material transit time.

The scan parameters vary slightly from vendor to vendor within the same scanner generation (e.g., 64-slice MDCT). The minimal equipment requirement for state-of-the-art coronary CTA is a 16-slice scanner. However, 40- or 64-slice MDCT scanners are recommended, as they increase

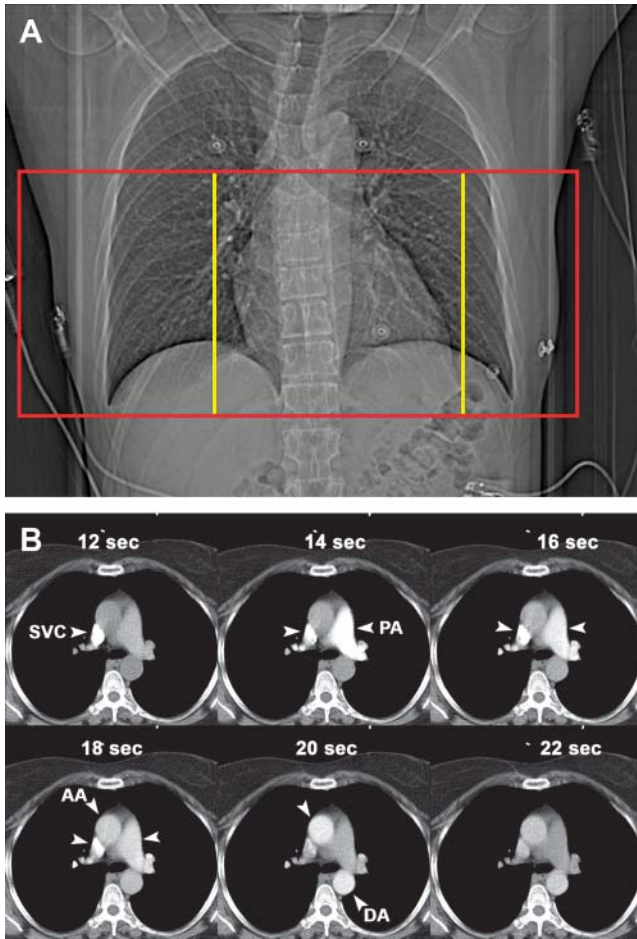


FIGURE 1. (A) Anteroposterior topogram showing volume coverage (field of view) required for dedicated coronary CTA (yellow box) and reading of incidental findings (red box). For coronary CTA, field of view extends from below tracheal bifurcation to base of heart. (B) Timing bolus image acquisition. Images at level of carina are acquired every 2 s starting 10 s after injection of 20 mL of iodinated contrast material. Arrowheads show passage of contrast material through superior vena cava (SVC) at 12 s, pulmonary artery (PA) at 14 s, and ascending aorta (AA) and descending aorta (DA) at 20 s. Coronary CTA scanning was started 20 s after initiation of contrast material injection.

the volume coverage and permit reduction of the scan time and the amount of contrast agent. In addition, these scanners provide thinner slice collimation and faster tube rotation, improving both spatial resolution and temporal resolution. Typical imaging parameters for 16- and 64-slice MDCT scanners are given in Table 2. The procedure, including patient preparation, premedication, and image acquisition, can be completed in 15 min.

Combined Studies for Chest Pain Evaluation in Emergency Departments

The fast volume coverage of 64-slice MDCT conceptually enables combined imaging of the coronary arteries, ascending aorta, and pulmonary arteries to assess for the presence of pulmonary embolism, thoracic aortic dissec-

TABLE 2
Technical Specifications of Imaging Protocols for Contrast-Enhanced Coronary Angiography by MDCT

Specification	Value for:	
	16-Slice scanner	64-Slice scanner
Tube current (mAs)	400–650	500–950
Tube voltage (kV)	120–140	120–140
Tube rotation time (ms)	375–500	330–420
Temporal resolution (ms)	183–250	165–210
Slice collimation (mm)	0.6–0.75	0.5–0.6
Scan length (s)	15–25	6–13
Contrast dose (mL)	70–100	50–80

tion, and CAD within a single CT examination. Compared with coronary CTA, this protocol requires an extension of the field of view and a prolonged administration of intravenous contrast material (20–25 s) to ensure adequate contrast enhancement of both the pulmonary and the thoracic aortic vasculature. For now, this concept is still preliminary, as data on the feasibility of this approach are not available. Specifically, it must be determined whether the diagnostic image quality of the coronary arteries can be maintained with this technique compared with standard coronary CTA before any further considerations are warranted.

Radiation Exposure

The effective radiation dose with coronary angiography by 64-slice MDCT is estimated to be approximately 11–22 mSv. However, ECG-controlled dose modulation is now available on most scanners. This method reduces the tube current during systole, resulting in a 30%–50% reduction in the effective radiation exposure (the effective radiation exposure with ECG-controlled dose modulation is 7–11 mSv, about 25% of the allowable yearly effective dose for radiation workers) (23,24). Dose modulation should be used in all patients with a regular low heart rate (sinus rhythm, <65 beats per minute, low heart rate variability, and absence of arrhythmia) (Fig. 2). This radiation exposure is comparable to 100–160 posteroanterior and lateral chest radiographs, or about 3 or 4 times the average yearly effective dose of natural background radiation (2.5 mSv). In comparison, diagnostic invasive selective coronary angiography has a mean effective radiation dose of 2.5–5 mSv, and nuclear perfusion imaging with SPECT has a mean effective radiation dose of ~15–20 mSv (25,26).

Image Reconstruction

Coronary CTA angiography scanning is performed in the spiral acquisition mode with continuous acquisition of data throughout the cardiac cycle. Multiple reconstruction parameters determine the quality of the reconstructed axial images.

Images usually are reconstructed with a slice thickness of 0.75 mm, 50% overlap between images (i.e., 0.4-mm

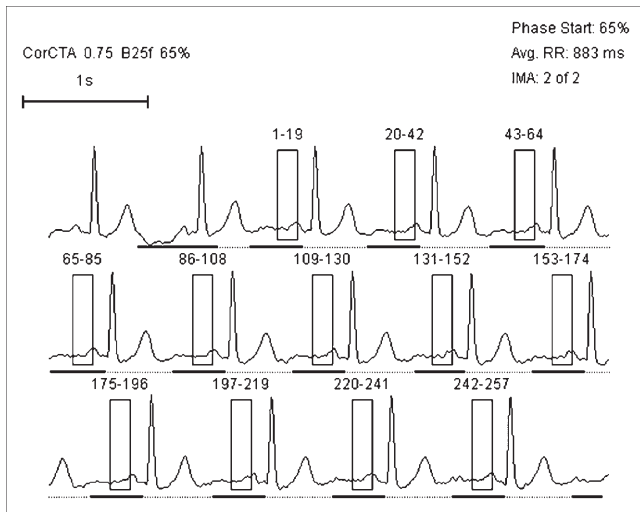


FIGURE 2. Retrospective ECG-gated reconstruction in patient with sinus rhythm (68 beats per minute), imaged with tube current modulation. White boxes indicate segment of R-R interval from which information will be used to reconstruct axial images. Bold white lines indicate time period of maximum tube current. In this patient, time used for image reconstruction starts at 65% of R-R interval and is well within time of tube current maximum. Tube current modulation should be used in patients with low and regular heart rates.

increment), and a pixel matrix of 512×512 . Although a thinner slice improves the resolution of the 3-dimensional dataset and the quality of reformatted images, it comes at the cost of increased image noise, which can significantly limit the diagnostic assessment of the coronary arteries in patients with a body mass index of greater than 30 kg/m^2 (3). In such patients, an increase in slice thickness to 1 mm may effectively reduce image noise (4).

Coronary CTA images typically are reconstructed with a medium smooth reconstruction kernel. Sharper reconstruction kernels can be applied for the tailored evaluation of coronary stents. A small field of view (18–20 cm) that encompasses only the heart is used for coronary CTA evaluation. For the assessment of incidental extracardiac findings, the raw data are reconstructed with a larger field of view (35 cm) and 3-mm-thick slices.

The use of retrospective ECG-gated reconstruction permits the reconstruction of complete datasets collected at different points of the R-R cycle. It has been shown that the optimal reconstruction window in which the coronary arteries can be visualized nearly free of motion artifacts starts in mid-diastole (60%–70% of the R-R interval) (27,28). Exceptions are patients with higher or irregular heart rates, in which a reconstruction window positioned in late systole (25%–35% of the R-R interval) often yields the best image quality. Although the half-scan algorithm (data from 210 degrees and 1 detector are used for a single image) is the default option for all patients with heart rates of less than 70 beats per minute, sometimes multisector reconstruction algorithms are used in patients with high heart rates. This technique can be applied retrospectively

and combines the information gathered by several detectors over 2–4 consecutive heartbeats at a single location to reconstruct an axial image. Although this approach improves temporal resolution up to 50 ms, so far there is only anecdotal evidence of its efficacy. Thus, it should be used only in cases in which the default reconstruction in various phases of the cardiac cycle does not provide sufficient image quality.

PITFALLS AND ARTIFACTS OF IMAGE EVALUATION

The coronary CTA dataset covering the entire volume of the heart contains as many as 500 axial images. A large number of axial images represents a challenge for the assessment and storage of CT datasets. Therefore, workstations used for the evaluation of coronary CTA provide multiple advanced image display methods that may facilitate the diagnostic evaluation.

Image Evaluation

Both axial images and multiplanar reformatted (MPR) images, which permit the visualization of the coronary arteries in multiple orientations orthogonal and perpendicular to the long axis of the vessel, are instrumental in detecting the presence of significant coronary artery stenosis. However, original axial images remain the cornerstone of the evaluation, as virtually all pathologies can be recognized (Fig. 3).

Once a suggestive location with luminal narrowing in the presence of calcified or noncalcified plaques has been identified on axial images, it is recommended that 2 long-axis views of the respective location be created with 3- to 5-mm thin-slab maximum-intensity-projection (MIP) images, which project the information of 4–7 original slices onto 1 image (Fig. 4). This technique enables the reconstruction of a true cross-sectional image of the vessel orthogonal to the long-axis view, which is similar to an intravascular ultrasound view. A comparison of the lumen at the location of narrowing with proximal and distal references enables a qualitative assessment of the degree of luminal narrowing.

An interactive evaluation with oblique MPR images and sliding thin-slab MIP (STS-MIP) images also has been proven helpful. Oblique MPR images are ideal for the confirmation of pathologic findings in the long and short axes of the vessel. STS-MIP images enhance the visualization of coronary artery stenosis in a long-axis view of the vessel if narrowing is caused by noncalcified atherosclerotic plaque.

STS-MIP images may not be used to evaluate the presence of stenosis in the short axis of the vessel and can cause false-positive readings in the presence of calcium.

In some cases with excellent image quality and the absence of severe calcification, a quantitative assessment similar to that of quantitative coronary angiography can be made and may improve diagnostic accuracy for the detection of significant stenosis. The direct measurement of lumen diameter can be helpful, especially for intermediate

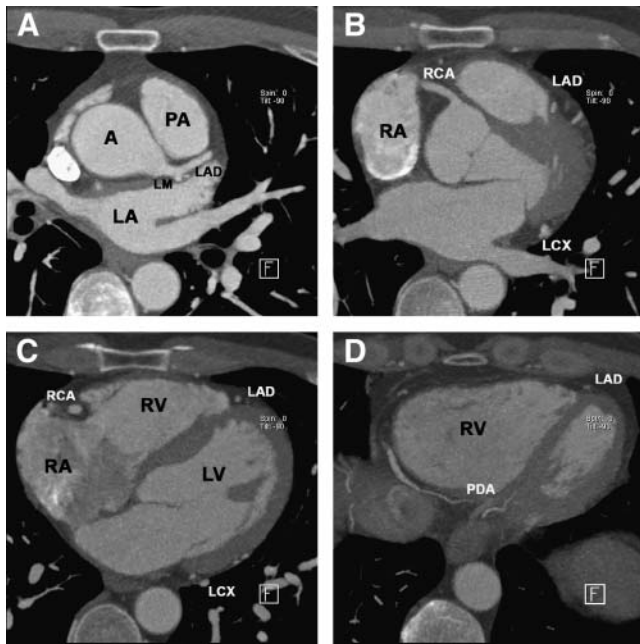


FIGURE 3. Patient with normal coronary morphology, as visualized by 64-slice MDCT. (A) Axial CT image was obtained at level of left main (LM) coronary artery ostium, which arises from left sinus of Valsalva and runs posterior to pulmonary artery (PA). LM coronary artery ostium divides into left anterior descending (LAD) and left circumflex (LCX) coronary arteries. A = aorta; LA = left atrium. (B) Axial CT image was obtained through origin of right coronary artery (RCA) at right aortic sinus and running between right ventricular outflow tract and right atrium (RA). Middle and distal segments of LAD coronary artery are located in interventricular groove. LCX coronary artery runs in left atrioventricular groove. (C) Cross-sectional view across midheart plane reveals middle RCA between RA and right ventricle (RV) and middle LAD coronary artery between RV and left ventricle (LV). (D) View of inferior aspect of heart shows posterior descending artery (PDA) arising from RCA running in posterior intraventricular groove.

lesions. Although software for automatic vessel border detection is available, manual correction or placement of the calipers should be performed at the proximal and distal reference sites as well as at the site of maximum luminal stenosis.

Prerendered images, such as curved MPR images, curved MIP images, and 3-dimensional volume-rendering technique images, can provide a general overview of the cardiac and coronary anatomy and can be prepared in a systematic fashion by supporting nonphysician staff. These images may be useful for portraying results to patients, referring physicians, or presentations but not for diagnostic purposes.

Stent Evaluation

Few data are available regarding the ability of MDCT to assess stent patency or in-stent restenosis. Even 64-slice MDCT scanners may be limited to stents with a diameter of more than 3 mm because of the high density of the stent, obscuring visualization inside the lumen, or the presence of beam-hardening artifacts from the stent struts (29,30).

Coronary Veins

It is important to be familiar with the venous anatomy, because a coronary vein can run parallel to or overlap a coronary artery and interfere with the evaluation of the coronary arteries, leading to pseudostenosis (e.g., anterior interventricular vein and left anterior descending artery or the intermediate branch).

Motion Artifacts

Because completely motion-free imaging of the coronary arteries requires a temporal resolution of 50 ms, motion artifacts occur at high rates and most often in the midsegment of the right coronary artery (Figs. 5A and 5B).

Misalignment and Slab Artifacts

Slab artifacts attributed to cardiac pulsation often degrade image quality (Fig. 5C). These artifacts occur especially in patients with high heart rates, heart rate variability, and the presence of irregular or ectopic heart beats (e.g., premature ventricular contractions [PVCs] and atrial fibrillation) and can be best recognized in a sagittal or coronal view. Thus, even with 64-slice scanners, a β -blocker should be used to reduce the heart rate to less than 65 beats per minute. These artifacts often limit the diagnostic assessment of coronary artery segments in patients with atrial fibrillation and frequent PVCs. One option is to reconstruct the dataset at different phases of the cardiac cycle. In general, reconstructions for coronary CTA are performed in mid-diastole to late diastole (60%–70% of the R-R interval). However, because the duration of diastole decreases as the heart rate increases, an end-systolic phase reconstruction at 25%–35% of the R-R interval may render the fewest artifacts. Also, temporal resolution may be enhanced by combining the projection data from consecutive heart cycles, that is, a multisector reconstruction algorithm (2–4 heart cycles, depending on the vendor) (18,19), which may eliminate slab artifacts. However, this reconstruction algorithm approach relies on the assumption that heart rate is regular throughout the scan acquisition, so that even small variations in the heart rate may degrade image quality. In the presence of PVCs, ECG editing (disabling or deleting the respective cardiac cycle) may improve image quality as long as there are sufficient overlap data (very low pitch used during cardiac imaging: 0.2–0.35).

Blooming Artifacts

High-attenuation structures, such as calcified plaques or stents, appear enlarged (or bloomed) because of partial-volume averaging effects and obscure the adjacent coronary lumen (Figs. 5D and 5E). Although sharper filters or kernels and thinner slices (0.5–0.6 mm) may reduce these artifacts and may enable an improved assessment of stent patency, they have little effect on calcified plaques. It is evident that severe coronary calcification is currently the major limiting factor; therefore, the elimination of calcium blooming artifacts is of utmost importance for the success of coronary CTA. In fact, the presence of dense calcified

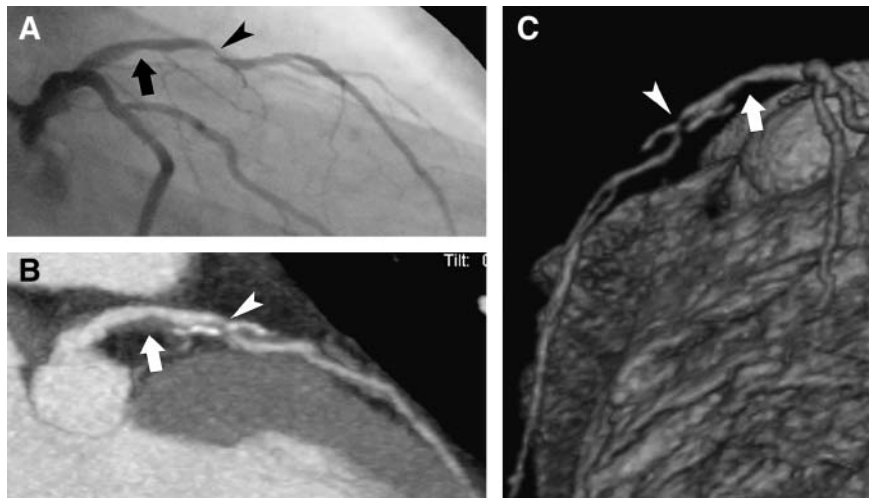


FIGURE 4. Stable angina and multiple cardiovascular risk factors in 66-y-old man. Images show detection of significant stenosis of middle segment of left anterior descending coronary artery (LAD) by MDCT and confirmation by coronary angiography. (A) Invasive selective coronary angiography demonstrates mild luminal narrowing in proximal LAD (arrow) and eccentric hemodynamically significant stenosis of middle LAD with residual filiform lumen (arrowhead). (B) Thin-slab MIP image across LAD plane shows large noncalcified plaque causing moderate (0%–30%) luminal obstruction in proximal LAD segment. Complex mixed coronary atherosclerotic plaque in middle LAD segment consists of both calcified plaque and noncalcified plaque, causing highly significant luminal narrowing. (C) 3-Dimensional volume-rendered CT image.

plaques is the main cause of false-positive results in coronary CTA because of overestimation of the degree of stenosis, potentially increasing the number of subjects undergoing both invasive selective coronary angiography and coronary CTA, especially in patient populations with a high prevalence of coronary calcification (11,28). A non-contrast calcium screening scan before coronary CTA (radiation exposure of approximately 1.3 mSv) could be performed to decide whether to perform subsequent coronary CTA. Although some authors have performed receiver operating characteristic analysis of their own data, which suggested a threshold for an Agatston score of greater than 1,000 to be linked to nondiagnostic examinations (14), this observation is limited, as no prospective evaluation has been performed. In fact, a single large calcified plaque in a proximal location may prevent the exclusion of significant coronary artery stenosis. Therefore, until the calcium blooming problem has been solved, the ability to safely exclude the presence of significant coronary artery stenosis remains limited in populations with a high prevalence of coronary calcification.

Beam-Hardening Artifacts

When an x-ray beam crosses a high-density structure, such as calcified plaque, a stent, or surgical clips, the majority of low-energy photons are absorbed. In the areas neighboring a dense structure, a high-energy beam passes through with little absorption, resulting in a low-density area in the reconstructed image. In general, beam-hardening artifacts occur only in 1 direction of the scan plane. However, it is important to recognize and distinguish these artifacts from noncalcified coronary atherosclerotic plaque.

Respiratory Artifacts

Respiratory artifacts produce “stair-step” artifacts through the entire dataset, including nonmoving structures, such as the bones. They can be recognized easily as inward motion of the sternum in a large sagittal view. Adequate

patient preparation with training of the breath-hold commands is mandatory to avoid such artifacts.

FINDINGS AND POTENTIAL CLINICAL APPLICATIONS

Detection of Significant Coronary Artery Stenosis

Over 35 studies with more than 1,500 patients have been performed to compare the diagnostic accuracies of electron-beam CT (EBCT) and MDCT for the detection of hemodynamically significant stenosis. Studies with EBCT and early versions of MDCT scanners, equipped with 4 detectors and a temporal resolution of 250–330 ms, demonstrated the ability of cardiac CT to detect significant coronary artery stenosis with moderate sensitivity and excellent specificity for both EBCT ($82\% \pm 6.4\%$ [mean \pm SD] and $87\% \pm 0.6\%$, respectively) and MDCT ($81\% \pm 7.2\%$ and $91\% \pm 0.9\%$, respectively) compared with selective x-ray coronary angiography (31).

The current generation of 64-slice MDCT scanners provides an in-plane resolution of 0.4 mm, a slice thickness of 0.6 mm, and a temporal resolution of 165 ms (32). The simultaneous acquisition of 64 parallel cross sections enables the imaging of the entire coronary artery tree in a single breath hold (~ 20 s for 16-slice MDCT versus ~ 10 s for 64-slice MDCT) (33).

Recent studies have reported excellent diagnostic accuracy for 64-slice MDCT in the detection of significant stenosis in smaller coronary artery segments and side branches as well (86%–94% sensitivity and 93%–97% specificity) (Fig. 4) (3,8,20,34). A high negative predictive value of 95%–97% suggests that 64-slice MDCT can reliably rule out the presence of hemodynamically significant CAD (3,8,20,34). The improvement is achieved through a significant decrease in the number of nonevaluable segments (7%), compared with 20% nonevaluable segments for 16-slice MDCT (35–41). The results also emphasize that low heart rates (<65 beats per minute)

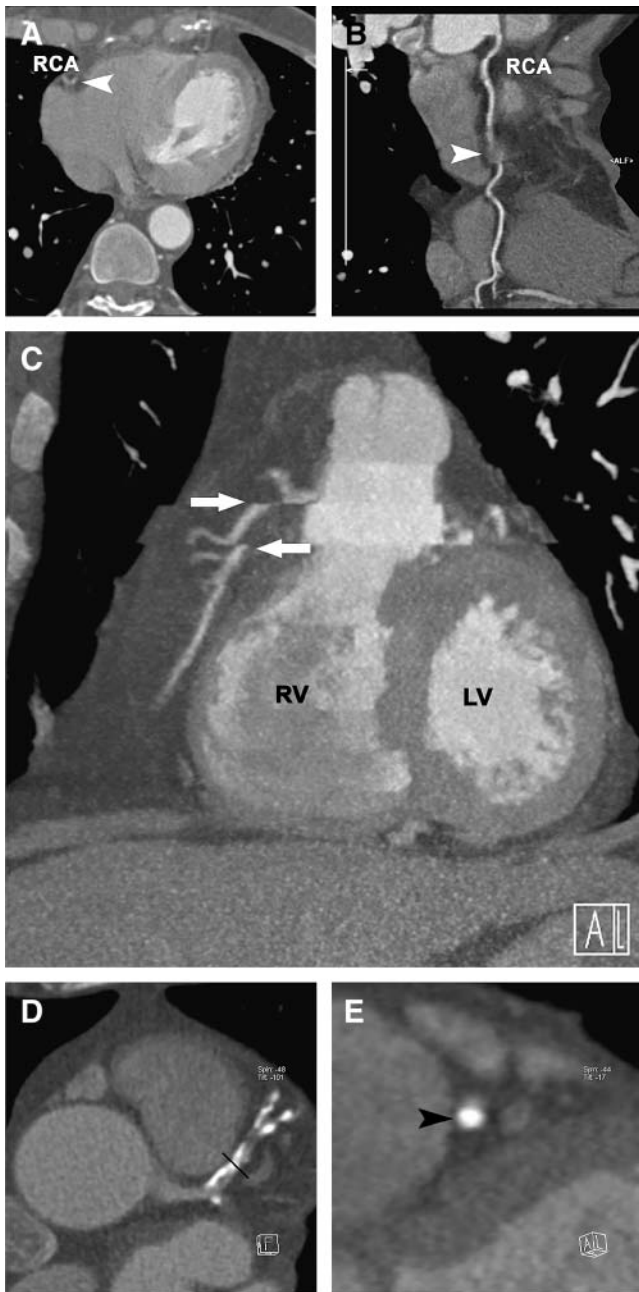


FIGURE 5. (A) Patient imaged at heart rate of 76 beats per minute. Axial image at level of middle right coronary artery (RCA) demonstrates typical “windmill” appearance of motion artifact (arrowhead). (B) Curved MPR image of entire length of RCA with motion artifact (arrowhead). (C) Patient with multiple extrasystolic beats during image acquisition. Stair-step artifacts (arrows) are caused by irregular rhythm and are best visualized in coronal view. Note that no irregularities occur at sternal border, excluding respiratory motion as cause of artifacts. LV = left ventricle; RV = right ventricle. (D and E) Increasing chest pain on exertion in 70-year-old man. (D) Axial image at level of left main coronary artery ostium and heavily calcified proximal and middle left anterior descending coronary artery. (E) Cross-sectional view at level of proximal left anterior descending coronary artery. Note blooming artifact (arrowhead) caused by vessel calcification, which precludes exclusion of significant coronary artery stenosis.

remain a prerequisite for excellent image quality in most patients (1).

Few studies have compared the degree of stenosis detected by quantitative coronary angiography with that detected by 16- or 64-slice CT (3,17,42,43). The overall correlation between the 2 methods appears to be moderate, even for selected segments with high image quality. The sensitivities of 64-slice MDCT for the detection of stenosis of less than 50%, stenosis of greater than 50%, and stenosis of greater than 75% have been reported to be 79%, 73%, and 80%, respectively, and the specificity has been reported to be 97% (44).

Detection and Characterization of Coronary Atherosclerotic Plaque

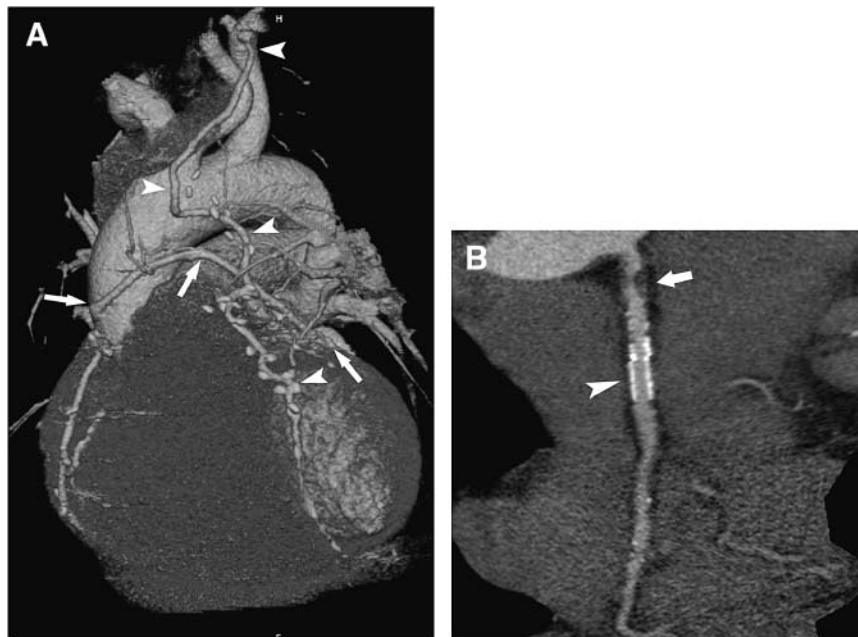
In addition to the delineation of the coronary artery lumen, cardiac MDCT also permits the visualization of coronary atherosclerotic plaque (45–47). There is growing evidence that the presence, amount, and composition of noncalcified coronary atherosclerotic plaque and the degree of coronary remodeling in proximal segments can be assessed by MDCT with a good correlation to intravascular ultrasound. MDCT accurately detects calcified or mixed plaque with sensitivities and specificities above 90%. However, MDCT is less accurate for the detection of noncalcified plaques, with sensitivities and specificities ranging from 60% to 85% (45,46), but has the potential to further stratify noncalcified plaque into fibrous plaque and lipid-rich plaque (48). The accuracy of MDCT, relative to intravascular ultrasound, in quantifying the volume of atherosclerotic plaque is moderate and depends greatly on plaque size and composition. Because of partial-volume effects, plaque detected by MDCT is overestimated, whereas smaller plaques (<0.5 mm) are not detected, leading to an underestimation of overall plaque volume. Two recent reports have indicated that the ability to determine plaque burden currently is hampered mainly by insufficient reproducibility and an interobserver variability for determining plaque volumes of up to 37% (44,49). Motion artifacts, low signal-to-noise ratio, and limited spatial resolution of MDCT account for most of the variability.

Potential Clinical Applications

Major limitations of the currently available data include the facts that all reports have been based on single-center experiences and that most studies have been conducted with a very specific subset of symptomatic middle-aged white men who had a high prevalence of CAD and who were already scheduled for invasive selective coronary angiography. Multicenter trials and studies with intermediate-risk populations are warranted.

Although the opportunity to noninvasively exclude significant CAD provides a compelling rationale for using coronary CTA in a variety of clinical applications, data on the clinical utility, cost, and cost-effectiveness, prerequisites to justifying clinical implementation, are not yet available. Two potential clinical applications are discussed here.

FIGURE 6. (A) 3-Dimensional volume-rendered image of patient showing status after left internal mammary graft to middle segment of left anterior descending coronary artery (arrowheads). Operative clips are visualized parallel to course of graft. In addition, venous coronary bypass graft can be seen between aorta and left circumflex coronary artery (arrows). (B) Curved MPR image with sharp image filter reconstruction of right coronary artery in patient with percutaneous stent placement (arrowhead). Lumen of stent (3.5-mm diameter) is patent. There is no evidence of in-stent restenosis or neointimal hyperplasia. In addition, this patient has large noncalcified plaque that protrudes into lumen of proximal right coronary artery, causing significant stenosis (arrow).



In 2001, 1.73 million coronary angiograms were performed for diagnostic purposes only. Because coronary angiography is associated with a small but not negligible risk of complications (inherent in invasive procedures), inconvenience to patients, and significant costs, coronary CTA may be an attractive alternative to invasive selective coronary angiography, with the potential to reduce the number of purely diagnostic angiograms. Patients with an intermediate likelihood of CAD (between 30% and 70% probability of having significant CAD, as determined by age, sex, and quality of chest pain) (50) may benefit from coronary CTA.

One of the most intriguing possibilities for coronary CTA is to improve the triage and management of patients with acute chest pain. Current triage of patients with chest pain but normal initial cardiac enzyme levels and nondiagnostic electrocardiograms is ineffective and does not provide information on the presence and extent of CAD. As a result of diagnostic uncertainty and the potentially fatal consequences of missed acute coronary syndrome (ACS) and associated malpractice costs annually, about 2.8 million patients with acute chest pain are admitted unnecessarily to the hospital, most of them being at very low risk for ACS (51–56). Because in most patients with ACS (80%–94%) significant coronary artery stenosis can be detected during invasive selective coronary angiography (57–59), coronary CTA, through exclusion of stenosis and plaque, may facilitate early triage and potentially decrease the number of hospital admissions for patients with acute chest pain.

Other potential applications include preoperative risk assessment, assessment of patency of stents placed in the left main coronary artery, and evaluation of bypass patency (Fig. 6).

Furthermore, the ability to detect and characterize the extent, distribution, and morphology of coronary atherosclerotic plaque may be useful for improving short- and long-term

cardiovascular risk stratification (60). However, because of the lack of any clinical data with respect to the assessment of noncalcified coronary atherosclerotic plaque by coronary CTA, the clinical significance of these findings is uncertain.

CONCLUSION

The current generation of 64-slice MDCT scanners with submillimeter slice collimation and high temporal resolution permits robust, fast, and reliable contrast-enhanced imaging of coronary arteries and coronary plaque. Adequate patient preparation and selection, including β -blocker administration in patients with high heart rates, optimized image reconstruction, and the availability of expert readers are prerequisites for obtaining diagnostic high-quality CT examinations. Severe coronary calcification remains the major limiting factor in coronary CTA.

Available data suggest that the high negative predictive value of 64-slice MDCT, relative to invasive selective coronary angiography, can rule out the presence of hemodynamically significant CAD. In addition, cardiac MDCT also permits the visualization of coronary atherosclerotic plaque with a good correlation to intracoronary ultrasound in examinations with high image quality.

Although data on clinical utility, cost, and cost-effectiveness are not yet available, coronary CTA may improve the management of patients with an intermediate probability of CAD and patients with acute chest pain.

REFERENCES

- Giesler T, Baum U, Ropers D, et al. Noninvasive visualization of coronary arteries using contrast-enhanced multidetector CT: influence of heart rate on image quality and stenosis detection. *AJR*. 2002;179:911–916.

2. Schroeder S, Kopp AF, Kuettner A, et al. Influence of heart rate on vessel visibility in noninvasive coronary angiography using new multislice computed tomography: experience in 94 patients. *Clin Imaging*. 2002;26:106–111.
3. Raff GL, Gallagher MJ, O'Neill WW, et al. Diagnostic accuracy of noninvasive coronary angiography using 64-slice spiral computed tomography. *J Am Coll Cardiol*. 2005;46:552–557.
4. Pena AJ, Moselewski F, Teague SD, et al. Heart rate variation during coronary multi-detector computed tomography: implication for imaging protocol optimization. Paper presented at: 6th International Conference on Cardiac CT; July 22, 2005; Boston, MA.
5. Nieman K, Rensing BJ, van Geuns RJ, et al. Non-invasive coronary angiography with multislice spiral computed tomography: impact of heart rate. *Heart*. 2002; 88:470–474.
6. Ropers D, Baum U, Pohle K, et al. Detection of coronary artery stenoses with thin-slice multi-detector row spiral computed tomography and multiplanar reconstruction. *Circulation*. 2003;107:664–666.
7. Ferencik M, Moselewski F, Ropers D, et al. Quantitative parameters of image quality in multidetector spiral computed tomographic coronary imaging with submillimeter collimation. *Am J Cardiol*. 2003;92:1257–1262.
8. Leber AW, Knez A, von Ziegler F, et al. Quantification of obstructive and nonobstructive coronary lesions by 64-slice computed tomography: a comparative study with quantitative coronary angiography and intravascular ultrasound. *J Am Coll Cardiol*. 2005;46:147–154.
9. Asselbergs FW, Monnick SH, Veeger NJ, et al. Coronary vasomotor response is related to the angiographic extent of coronary sclerosis in patients with stable angina pectoris. *Clin Sci (Lond)*. 2004;106:115–120.
10. Silber S. Nitrates: why and how should they be used today? Current status of the clinical usefulness of nitroglycerin, isosorbide dinitrate and isosorbide-5-mononitrate. *Eur J Clin Pharmacol*. 1990;38(suppl 1):S35–S51.
11. Hoffmann U, Moselewski F, Cury RC, et al. Predictive value of 16-slice multidetector spiral computed tomography to detect significant obstructive coronary artery disease in patients at high risk for coronary artery disease: patient- versus segment-based analysis. *Circulation*. 2004;110:2638–2643.
12. Kajinami K, Seki H, Takekoshi N, et al. Noninvasive prediction of coronary atherosclerosis by quantification of coronary artery calcification using electron beam computed tomography: comparison with electrocardiographic and thallium exercise stress test results. *J Am Coll Cardiol*. 1995;26:1209–1221.
13. Kuettner A, Beck T, Drosch T, et al. Diagnostic accuracy of noninvasive coronary imaging using 16-detector slice spiral computed tomography with 188 ms temporal resolution. *J Am Coll Cardiol*. 2005;45:123–127.
14. Kuettner A, Trabold T, Schroeder S, et al. Noninvasive detection of coronary lesions using 16-detector multislice spiral computed tomography technology: initial clinical results. *J Am Coll Cardiol*. 2004;44:1230–1237.
15. Achenbach S, Ropers D, Pohle FK, et al. Detection of coronary artery stenoses using multi-detector CT with 16×0.75 collimation and 375 ms rotation. *Eur Heart J*. 2005;26:1978–1986.
16. Martuscelli E, Romagnoli A, D'Eliseo A, et al. Accuracy of thin-slice computed tomography in the detection of coronary stenoses. *Eur Heart J*. 2004;25:1043–1048.
17. Morgan-Hughes GJ, Roobottom CA, Owens PE, Marshall AJ. Highly accurate coronary angiography with submillimetre, 16 slice computed tomography. *Heart*. 2005;91:308–313.
18. Dewey M, Laule M, Krug L, et al. Multisegment and halfscan reconstruction of 16-slice computed tomography for detection of coronary artery stenoses. *Invest Radiol*. 2004;39:223–229.
19. Hoffmann MH, Shi H, Schmitz BL, et al. Noninvasive coronary angiography with multislice computed tomography. *JAMA*. 2005;293:2471–2478.
20. Leschka S, Alkadhi H, Plass A, et al. Accuracy of MSCT coronary angiography with 64-slice technology: first experience. *Eur Heart J*. 2005;26:1482–1487.
21. Mollet NR, Cademartiri F, Krestin GP, et al. Improved diagnostic accuracy with 16-row multi-slice computed tomography coronary angiography. *J Am Coll Cardiol*. 2005;45:128–132.
22. Mollet NR, Cademartiri F, Nieman K, et al. Multislice spiral computed tomography coronary angiography in patients with stable angina pectoris. *J Am Coll Cardiol*. 2004;43:2265–2270.
23. Siemens A. *SOMATOM Sensation Cardiac 64: Application Guide*. Forchheim, Germany: Siemens AG Medical Solutions; 2004.
24. Hundt W, Rust F, Stabler A, et al. Dose reduction in multislice computed tomography. *J Comput Assist Tomogr*. 2005;29:140–147.
25. Morin RL, Gerber TC, McCollough CH. Radiation dose in computed tomography of the heart. *Circulation*. 2003;107:917–922.
26. Herzog C, Abolmaali N, Balzer JO, et al. Heart-rate-adapted image reconstruction in multidetector-row cardiac CT: influence of physiological and technical prerequisite on image quality. *Eur Radiol*. 2002;12:2670–2678.
27. Sanz J, Rius T, Kuschnir P, et al. The importance of end-systole for optimal reconstruction protocol of coronary angiography with 16-slice multidetector computed tomography. *Invest Radiol*. 2005;40:155–163.
28. Halliburton SS, Petersilka M, Schwartzman PR, et al. Evaluation of left ventricular dysfunction using multiphase reconstructions of coronary multi-slice computed tomography data in patients with chronic ischemic heart disease: validation against cine magnetic resonance imaging. *Int J Cardiovasc Imaging*. 2003;19:73–83.
29. Gaspar T, Halon DA, Lewis BS, et al. Diagnosis of coronary in-stent restenosis with multidetector row spiral computed tomography. *J Am Coll Cardiol*. 2005; 46:1573–1579.
30. Maintz D, Seifarth H, Raupach R, et al. 64-Slice multidetector coronary CT angiography: in vitro evaluation of 68 different stents. *Eur Radiol*. 2006;16:818–826.
31. Hoffmann U, Dunn JH, d'Janne E, Othee B. Is CT angiography ready for prime time? A meta-analysis [abstract]. *J Am Coll Cardiol*. 2004;43(suppl A):312A.
32. Flohr T, Bruder H, Stierstorfer K, et al. New technical developments in multislice CT, part 2: sub-millimeter 16-slice scanning and increased gantry rotation speed for cardiac imaging. *Rofo*. 2002;174:1022–1027.
33. Ferencik M, Moselewski F, Ropers D, et al. Quantitative parameters of image quality in multidetector spiral computed tomographic coronary imaging with submillimeter collimation. *Am J Cardiol*. 2003;92:1257–1262.
34. Mollet NR, Cademartiri F, van Mieghem CA, et al. High-resolution spiral computed tomography coronary angiography in patients referred for diagnostic conventional coronary angiography. *Circulation*. 2005;112:2318–2323.
35. Achenbach S, Giesler T, Ropers D, et al. Detection of coronary artery stenoses by contrast-enhanced, retrospectively electrocardiographically-gated, multislice spiral computed tomography. *Circulation*. 2001;103:2535–2538.
36. Achenbach S, Moshage W, Ropers D, et al. Value of electron-beam computed tomography for the noninvasive detection of high-grade coronary-artery stenoses and occlusions. *N Engl J Med*. 1998;339:1964–1971.
37. Becker CR, Knez A, Leber A, et al. Detection of coronary artery stenoses with multislice helical CT angiography. *J Comput Assist Tomogr*. 2002;26:750–755.
38. Flohr T, Ohnesorge B. Heart rate adaptive optimization of spatial and temporal resolution for electrocardiogram-gated multislice spiral CT of the heart. *J Comput Assist Tomogr*. 2001;25:907–923.
39. Kopp AF, Schroeder S, Kuettner A, et al. Non-invasive coronary angiography with high resolution multidetector-row computed tomography: results in 102 patients. *Eur Heart J*. 2002;23:1714–1725.
40. Kopp AF, Schroeder S, Kuettner A, et al. Coronary arteries: retrospectively ECG-gated multi-detector row CT angiography with selective optimization of the image reconstruction window. *Radiology*. 2001;221:683–688.
41. Ohnesorge B, Flohr T, Becker C, et al. Cardiac imaging by means of electrocardiographically gated multislice spiral CT: initial experience. *Radiology*. 2000;217:564–571.
42. Cury RC, Pomerantsev EV, Ferencik M, et al. Comparison of the degree of coronary stenoses by multidetector computed tomography versus by quantitative coronary angiography. *Am J Cardiol*. 2005;96:784–787.
43. Kefer J, Coche E, Legros G, et al. Head-to-head comparison of three-dimensional navigator-gated magnetic resonance imaging and 16-slice computed tomography to detect coronary artery stenosis in patients. *J Am Coll Cardiol*. 2005;46:92–100.
44. Leber AW, Becker A, Knez A, et al. Accuracy of 64-slice computed tomography to classify and quantify plaque volumes in the proximal coronary system: a comparative study using intravascular ultrasound. *J Am Coll Cardiol*. 2006;47: 672–677.
45. Leber AW, Knez A, Becker A, et al. Accuracy of multidetector spiral computed tomography in identifying and differentiating the composition of coronary atherosclerotic plaques: a comparative study with intracoronary ultrasound. *J Am Coll Cardiol*. 2004;43:1241–1247.
46. Achenbach S, Moselewski F, Ropers D, et al. Detection of calcified and noncalcified coronary atherosclerotic plaque by contrast-enhanced, submillimeter multidetector spiral computed tomography: a segment-based comparison with intravascular ultrasound. *Circulation*. 2004;109:14–17.
47. Achenbach S, Giesler T, Ropers D, et al. Comparison of image quality in contrast-enhanced coronary-artery visualization by electron beam tomography and retrospectively electrocardiogram-gated multislice spiral computed tomography. *Invest Radiol*. 2003;38:119–128.
48. Leber AW, Knez A, White CW, et al. Composition of coronary atherosclerotic plaques in patients with acute myocardial infarction and stable angina pectoris determined by contrast-enhanced multislice computed tomography. *Am J Cardiol*. 2003;91:714–718.
49. Ferencik M, Nieman K, Achenbach S. Noncalcified and calcified coronary plaque detection by contrast-enhanced multi-detector computed tomography: a study of interobserver agreement. *J Am Coll Cardiol*. 2006;47:207–209.

50. Gibbons RJ, Chatterjee K, Daley J, et al. ACC/AHA/ACP-ASIM guidelines for the management of patients with chronic stable angina: a report of the American College of Cardiology/American Heart Association Task Force on Practice Guidelines (Committee on Management of Patients With Chronic Stable Angina). *J Am Coll Cardiol.* 1999;33:2092–2197.
51. McCarthy BD, Beshansky JR, D'Agostino RB, et al. Missed diagnoses of acute myocardial infarction in the emergency department: results from a multicenter study. *Ann Emerg Med.* 1993;22:579–582.
52. Lee TH, Cook EF, Weisberg M, et al. Acute chest pain in the emergency room: identification and examination of low-risk patients. *Arch Intern Med.* 1985; 145:65–69.
53. Solinas L, Raucci R, Terrazzino S, et al. Prevalence, clinical characteristics, resource utilization and outcome of patients with acute chest pain in the emergency department: a multicenter, prospective, observational study in northeastern Italy. *Ital Heart J.* 2003;4:318–324.
54. McCaig LF, Burt CW. National Hospital Ambulatory Medical Care Survey: 2002 emergency department summary. *Adv Data.* 2004;Mar 18:1–34.
55. Pope JH, Aufderheide TP, Ruthazer R, et al. Missed diagnoses of acute cardiac ischemia in the emergency department. *N Engl J Med.* 2000;342:1163–1170.
56. Prina LD, Decker WW, Weaver AL, et al. Outcome of patients with a final diagnosis of chest pain of undetermined origin admitted under the suspicion of acute coronary syndrome: a report from the Rochester Epidemiology Project. *Ann Emerg Med.* 2004;43:59–67.
57. Roe MT, Harrington RA, Prosper DM, et al. Clinical and therapeutic profile of patients presenting with acute coronary syndromes who do not have significant coronary artery disease. The Platelet Glycoprotein IIb/IIIa in Unstable Angina: Receptor Suppression Using Integrilin Therapy (PURSUIT) Trial Investigators. *Circulation.* 2000;102:1101–1106.
58. Wallentin L. Non-ST-elevation acute coronary syndrome: fuel for the invasive strategy. *Lancet.* 2002;360:738–739.
59. Wallentin L, Lagerqvist B, Husted S, et al. Outcome at 1 year after an invasive compared with a non-invasive strategy in unstable coronary-artery disease: the FRISC II invasive randomised trial. FRISC II Investigators. Fast Revascularisation during Instability in Coronary artery disease. *Lancet.* 2000;356: 9–16.
60. Achenbach S, Ropers D, Hoffmann U, et al. Assessment of coronary remodeling in stenotic and nonstenotic coronary atherosclerotic lesions by multidetector spiral computed tomography. *J Am Coll Cardiol.* 2004;43:842–847.

Erratum

In the article “Analysis of ^{18}F -FET PET for Grading of Recurrent Gliomas: Is Evaluation of Uptake Kinetics Superior to Standard Methods?” by Pöpperl et al. (*J Nucl Med.* 2006;47:393–403), the first equation on page 396 contained an error. The authors regret the error and provide the corrected equation below:

$$\sum_{i=13}^{16} w_i \times (n_i - n_{i-1}) \quad \text{with} \quad w_i = \frac{d_i + d_{i-1}}{2}$$